1991ApJ...377..629L

THE ASTROPHYSICAL JOURNAL, 377:629–638, 1991 August 20
© 1991. The American Astronomical Society. All rights reserved. Printed in U.S.A.

OBSERVATIONS OF STELLAR WINDS FROM HOT STARS AT 1.3 MILLIMETERS[1]

CLAUS LEITHERER[2]
Space Telescope Science Institute,[3] 3700 San Martin Drive, Baltimore, Maryland 21218
AND
CARMELLE ROBERT[4]
Département de Physique, Université de Montréal and Observatoire du mont Mégantic, Montréal, Québec, Canada
Received 1990 December 21; accepted 1991 February 25

ABSTRACT

We report the detection of seven hot stars at a wavelength of 1.3 mm with the Swedish-ESO Submillimeter Telescope at La Silla. The measured millimeter fluxes are combined with existing centimeter data to study the radio spectrum. The spectral index of $\sim$0.6 is consistent with emission from optically thick free-free radiation in an isotropic, isothermal outflow expanding at constant velocity. We discuss several mechanisms which can lead to spectral indices different from 0.6. In particular, we focus on the influence of acceleration and deceleration zones and on changes of the ionization structure in the wind. Such effects are likely to be present and may steepen the spectral index by $\sim$0.1. However, the consequences for the derived mass-loss rates if these effects are not taken into account are negligible. Our results suggest that radio mass-loss rates are not significantly affected by uncertainties due to extrapolation of the wind conditions from regions where spectral lines are formed to the region where the radio flux is emitted.

Subject headings: stars: early-type — stars: mass loss — stars: radio radiation — stars: winds

1. INTRODUCTION

Hot luminous stars develop strong stellar winds with terminal velocities v_∞ far exceeding the photospheric surface escape velocity and with mass-loss rates $\dot{M}$ high enough to decrease the stellar mass significantly on an evolutionary time scale (Cassinelli & Lamers 1987; Willis & Garmany 1987). Determination of accurate mass-loss rates—although crucial for comparison with theoretical models—is far from trivial, and even the best mass-loss rates derived so far have uncertainties of about a factor of 2 (see Lamers 1988 for a discussion of the uncertainties).

Radio measurements at centimeter wavelengths have provided the most reliable mass-loss rates (Abbott et al. 1980; Abbott, Bieging, and Churchwell 1981; Abbott et al. 1986; Bieging, Abbott, and Churchwell 1989). Stellar winds expanding at constant velocity give rise to a characteristic $S_\nu \propto \nu^{0.6}$ spectrum due to optically thick emission from thermal bremsstrahlung (Panagia & Felli 1975; Wright & Barlow 1975; Olnon 1975). The simplicity of the radiative transfer of the free-free emission process makes only few model assumptions necessary when $\dot{M}$ is determined.

A major uncertainty inherent in $\dot{M}$ derived from centimeter data is introduced by the lack of reliable velocity determinations for the wind region emitting centimeter radiation. Typically, radiation observed at a wavelength at 6 cm is emitted at about 10^2–10^3 stellar radii (Lamers 1988). In order to transform the observed wind density into a mass-loss rate, an assumption on the velocity must be made. Usually, the velocity v_∞ measured in UV resonance lines, which represents the flow velocity at about 10 stellar radii, is extrapolated to the region observed at centimeter wavelengths assuming $v_\infty =$ constant. A second complication is due to the uncertain ionization state of the wind—in particular if Wolf-Rayet (W-R) stars are considered. Ionization conditions are inferred from spectral line analyses close to the stellar surface. Assumptions on the thermal equilibrium must be made to extrapolate the physical conditions prevailing in the line-emitting region to the wind region where the centimeter flux originates.

Thermal millimeter radiation is emitted by the same process as radiation observed at centimeter wavelengths. However, due to the frequency dependence of the free-free opacity, millimeter radiation originates where UV resonance lines and some strong optical recombination lines are formed. Hence, the free-free spectrum from $\sim$1 mm to $\sim$6 cm samples wind regions between $\sim$10 and $\sim 10^3$ stellar radii, and model assumptions on the density and ionization structure in these regions can be tested. Recent advances in telescope and detector technology have made it possible to measure some of the strongest hot stars at millimeter wavelengths. In this paper we report on the detection of a sample of hot luminous stars at 1.3 mm and discuss the implications for the derived stellar-wind properties.

2. OBSERVATIONS

We observed a sample of hot luminous stars with the 15 m Swedish-ESO Submillimeter Telescope (SEST) at ESO, La Silla, during 1990 September 12–14, using the bolometer of the MPIfR (Kreysa 1990). The observations were carried out at a frequency of 230 GHz (corresponding to a wavelength of 1.3 mm). The beam size was 25″. SEST is not equipped with a chopping secondary. Therefore chopping must be done with a focal plane chopper (Kreysa 1990). For our observations the chopper was operated at 8 Hz and 105″ throw in azimuth. The observing technique consisted of the standard beam-switching method performing ON-ON measurements on the position of the

[1] Based on observations made at the European Southern Observatory, La Silla.

[2] Affiliated with the Astrophysics Division of the Space Science Department of ESA.

[3] Operated by the Association of Universities for Research in Astronomy, Inc. under contract with the National Aeronautics and Space Administration.

[4] Postal address: Space Telescope Science Institute, 3700 San Martin Drive, Baltimore, MD 21218.

© American Astronomical Society • Provided by the NASA Astrophysics Data System

program stars. The telescope pointing was checked with bright 1.3 mm standards before slewing to the expected position of the program stars and immediately afterward. If the total time spent on one object exceeded about 1 hr, the observations of the program star were interrupted to perform an additional pointing check before returning to the original star. Beam switching was done by moving the telescope in azimuth by 105″ after integration of 10 s in one beam. One complete measurement of an object (which is referred to as a "scan") consisted of 10 such ON-ON sequences with 10 s spent in each beam. Thus the total on-target time per scan was 200 s. The program stars are located in H II regions which might be expected to contaminate the stellar radio fluxes. Control measurements at offset positions 30″ away from the stellar coordinates were performed to verify that the detections were not affected by resolved nebular emission. No significant flux was detected at the offset positions.

The atmospheric transmission was measured every 1–2 hr by skydips. The optical depth at 1.3 mm varied between 0.05 and 0.15 during the observing period. Conversion to absolute fluxes was done using Uranus as a calibration standard. Uranus is essentially a point source at the resolution of SEST at 1.3 mm. We adopted a brightness temperature of 101 K at 1.3 mm for Uranus (Ulich, Dickel, & de Pater 1984). Uranus subtended a solid angle of 2.48×10^{-10} sr at the epoch of the observations. After a small correction for beam-size effects (Chini, private communication) we obtain a flux density of 38 Jy at 230 GHz for Uranus.

Table 1 summarizes the most important observational data. Column (1) gives the HD numbers for all objects observed. Other well-known designations for some of the stars are HD 37128 = ϵ Ori, HD 50896 = EZ CMa, HD 66811 = ζ Pup, HD 68273 = γ^2 Vel, and HD 152236 = ζ^1 Sco. The flux measurements were done with the telescope pointing at the optical positions (col. [2] and [3]) which agree with the radio positions measured at centimeter wavelengths (Abbott et al. 1980, 1986[5]; Bieging et al. 1989). The counts obtained for each scan were converted into flux units after correction for air mass and variations of the atmospheric transmission with time. No correction for the variation of gain with elevation has been applied since this effect is small as compared to variations of the atmospheric transmission. Individual scans of each object were averaged, and the standard deviation of the mean was calculated. The measured flux densities at 230 GHz together with the statistical 1 σ errors are in column (4) of Table 1.

[5] Note the typographical error in the optical position of HD 68273 in Table 1 of Abbott et al. (1986).

3. MEASUREMENT OF THE SPECTRAL INDEX

We selected only program stars which had already been detected at centimeter wavelengths in order to maximize the detection probability at 1.3 mm. Therefore our sample is biased toward the radio-brightest hot stars. Objects known as nonthermal radio sources at centimeter wavelengths were excluded.

Most radio measurements obtained previously were restricted to the wavelength region between 2 and 6 cm. Due to the small wavelength baseline, derivation of radio spectral indices from centimeter data only is relatively uncertain. Combining centimeter and millimeter data reduces the uncertainty in the derived spectral index significantly. We searched through the literature to collect as many radio data as possible for the seven program stars. A weighted linear fit to all data, including our millimeter measurements, was performed, and the slope α of the free-free spectrum was derived. We define α by

$$\alpha = \frac{d \log S_\nu}{d \log \nu}, \quad (1)$$

where S_ν is the free-free flux observed at frequency ν. The values derived for the spectral index are listed in column (5) of Table 1.

HD 37128—Only one measurement at 6 cm has been published so far (Abbott et al. 1980). We derive $\alpha = 0.55 \pm 0.09$ (Fig. 1). Abbott et al. reported the presence of blurring in their synthesized VLA image of this star due to phase errors. An independent measurement at centimeter wavelengths would be desirable to confirm the spectral index.

HD 50896—This star has been extensively monitored by Hogg (1989). No significant flux variation over a time scale of years has been found. Radio data at 4.9, 15, 22.5, and 230 GHz are consistent with a spectral index $\alpha = 0.64 \pm 0.06$ (Fig. 2).

HD 66811—Bieging et al. (1989) detected HD 66811 at 15 and 4.9 GHz. Combining their data with our millimeter flux leads to a spectral index of $\alpha = 0.71 \pm 0.03$ (Fig. 3).

HD 68273—Due to its proximity to the Sun and its dense wind, HD 68273 is the strongest thermal radio source among hot luminous stars. A large number of individual radio measurements have been published (see Fig. 4). Our fit of $\alpha = 0.67 \pm 0.02$ is based on all data points in Figure 4 except those published by Purton et al. (1982). Interferometric measurements revealed a nonthermal source at a distance of $\sim 2'$ from HD 68273 (Jones 1985) which may effect the low-resolution data of Purton et al. (1982).

HD 151932—Comparison of the centimeter data published by Abbott et al. (1986) and Hogg (1989) suggests variability of

TABLE 1

OBSERVATIONAL DATA

Object (1)	R.A. (1950) (2)	Decl. (1950) (3)	Flux Density (4)	Spectral Index (5)
HD 37128	05^{h}33^{m}40^s.5	−01°13′56″	13.1 ± 2.2	0.55 ± 0.09
HD 50896	06 52 08.1	−23 51 52	14.1 ± 3.1	0.64 ± 0.06
HD 66811	08 01 49.5	−39 51 40	20.2 ± 1.8	0.71 ± 0.03
HD 68273	08 07 59.5	−47 11 18	342 ± 27	0.67 ± 0.02
HD 151932	16 48 48.4	−41 46 17	11.6 ± 2.3	0.55 ± 0.06
HD 152236	16 50 27.7	−42 16 51	23.0 ± 2.4	0.63 ± 0.04
HD 152408	16 51 28.8	−41 04 16	14.7 ± 3.1	0.68 ± 0.06

© American Astronomical Society • Provided by the NASA Astrophysics Data System

1991ApJ...377..629L

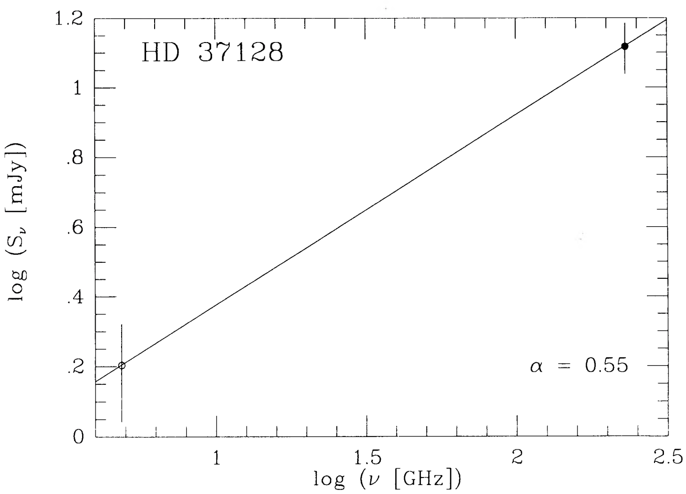

FIG. 1.—Observed radio spectrum of HD 37128 from 6 to 1.3 mm. Filled circle: our millimeter data; open circle: Abbott et al. (1980). Solid line is a linear fit to the observations. Spectral index: 0.55 ± 0.09.

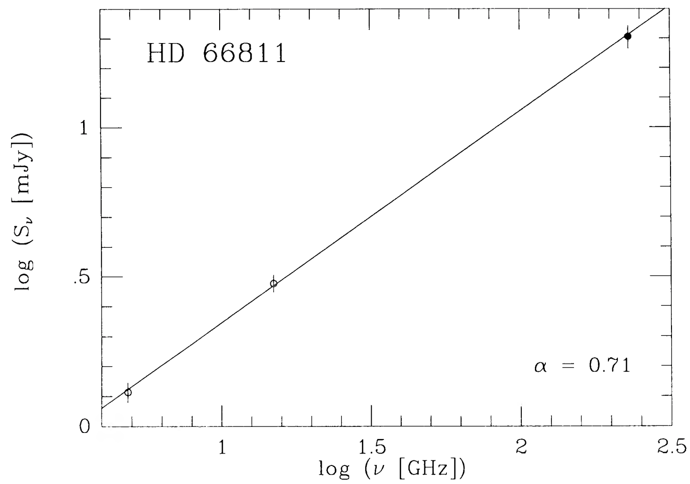

FIG. 3.—Same as Fig. 1 but for HD 66811. Filled circle: our millimeter data; open circles: Bieging et al. (1989). Spectral index 0.71 ± 0.03.

HD 151932 at the 30% level (Fig. 5). The spectral index we derive ($\alpha = 0.55 \pm 0.06$) may be affected by such variability. Our fit is based on the mean of all flux values given by Abbott et al. and Hogg at one frequency.

HD 152236—Our millimeter data and the centimeter measurements of Bieging et al. (1989) give $\alpha = 0.63 \pm 0.04$ (Fig. 6). Note that Bieging et al. measured $S_\nu = 1.2$ mJy at 4.9 GHz in 1981 whereas their multifrequency data of 1984 give $S_\nu = 1.9$ mJy at the same frequency. We did not include the former measurement in our spectral index fit since only one frequency point was measured in 1981. It is not clear if the flux variation is due to intrinsic variation of the wind or to poor accuracy of the data.

HD 152408—The spectral index derived from the millimeter data and centimeter data by Bieging et al. (1989) is $\alpha = 0.68 \pm 0.06$ (Fig. 7).

The errors associated with the spectral indices include only the formal errors resulting from the fit. The principal uncertainty of the 1.3 mm fluxes is due to measurement errors, which are of the order 10%–25%. Systematic errors due to uncertainties in the absolute flux calibration are difficult to assess in a quantitative way. They are probably on the order of $\sim 10\%$ (Chini 1991, private communication; de Pater 1991, private communication). Any revision of the absolute flux scale at 1.3 mm would change the derived spectral indices accordingly. We will address the significance of such systematic effects for the derived mass-loss rates in the following section.

4. MASS-LOSS RATES FROM 1.3 mm FLUXES

Panagia & Felli (1975) and Wright & Barlow (1975) developed a relation between the measured radio flux and the wind properties. For an isothermal, spherically symmetric, stationary outflow at constant velocity they find

$$S_\nu = 2.32 \times 10^4 \left(\frac{\dot{M}Z}{v_\infty \mu}\right)^{4/3} \left(\frac{\gamma g_\nu \nu}{d^3}\right)^{2/3} , \qquad (2)$$

where S_ν is the radio flux in mJy measured at frequency ν in Hz; $\dot{M}$ is in $M_\odot$ yr^{-1}; v_∞ is in km s^{-1}; μ, Z, and γ are the mean molecular weight, the rms ionic charge, and the number of

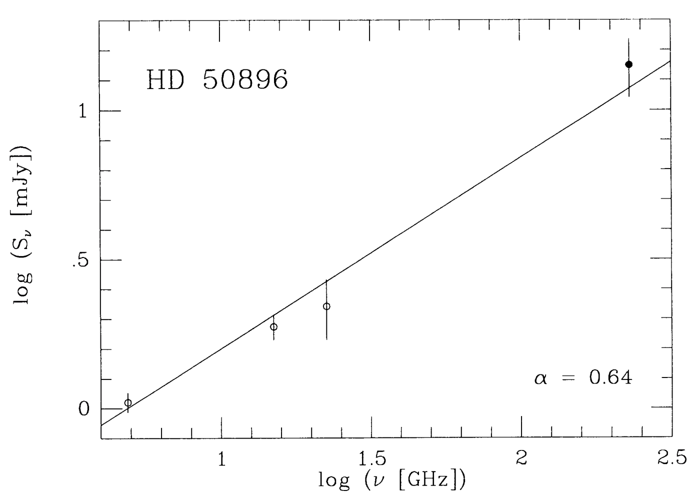

FIG. 2.—Same as Fig. 1 but for HD 50896. Filled circle: our millimeter data; open circles: Hogg (1989). Spectral index: 0.64 ± 0.06.

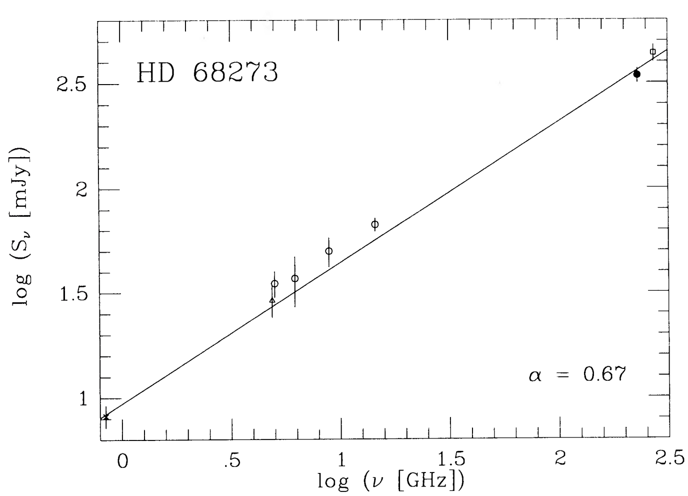

FIG. 4.—Same as Fig. 1 but for HD 68273. (Note the extended frequency range in this figure to include the Jones (1985) 0.84 GHz data point at 8.2 ± 1.0 mJy.) Filled circle: our millimeter data; open circles: Purton et al. (1982); open triangle: Hogg (1985), error estimated; open square: Williams et al. (1990); cross: Jones (1985). Measurements of Purton et al. were excluded from the linear fit (*see text*). Spectral index: 0.67 ± 0.02.

© American Astronomical Society • Provided by the NASA Astrophysics Data System

1991ApJ...377..629L

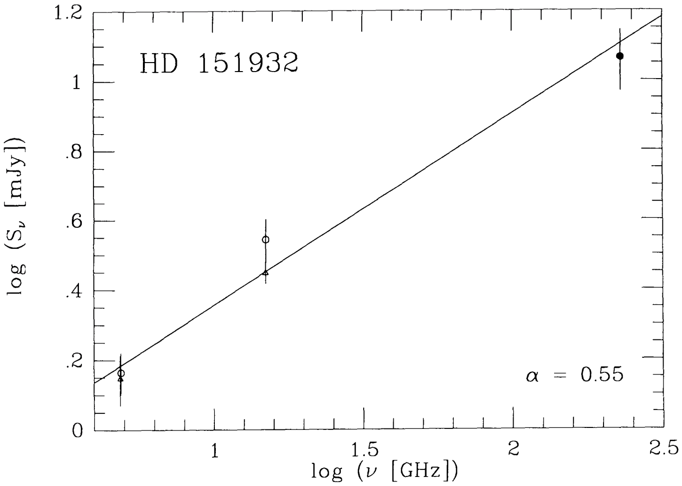

FIG. 5.—Same as Fig. 1 but for HD 151932. Filled circle: our millimeter data; open circles: Hogg (1989); open triangles: Abbott et al. (1986). Spectral index: 0.55 ± 0.06.

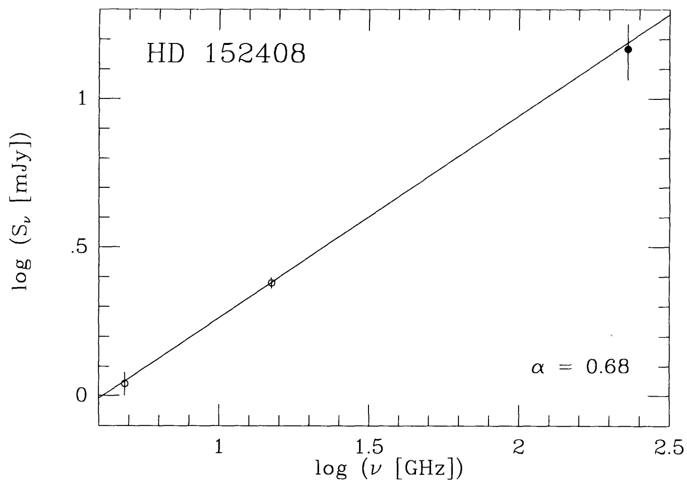

FIG. 7.—Same as Fig. 1 but for HD 152408. Filled circle: our millimeter data; open circles: Bieging et al. (1989). Spectral index: 0.68 ± 0.06.

electrons per ion, respectively; and d is the distance in kpc. The free-free Gaunt factor is given by g_ν, which can be approximated as

$$g_\nu = 9.77\left(1 + 0.13 \log \frac{T_e^{3/2}}{Z\nu}\right) \quad (3)$$

(Abbott et al. 1986; see also Appendix). The electron temperature of the wind is given by T_e. Except for the very weak T_e dependence of the Gaunt factor, equation (2) is independent of the electron temperature. Since $g_\nu \propto \nu^{-0.1}$ at centimeter and millimeter wavelengths, equation (2) predicts a characteristic radio spectral index of approximately 0.6. This theoretical index is consistent with the average observed α derived in the previous section. In the following we will assume that the model used for deriving equation (2) is correct and determine mass-loss rates from 1.3 millimeter fluxes with this relation. Subsequently we will study the consequences for the theoretical radio spectra of individual stars if some model assumptions are varied.

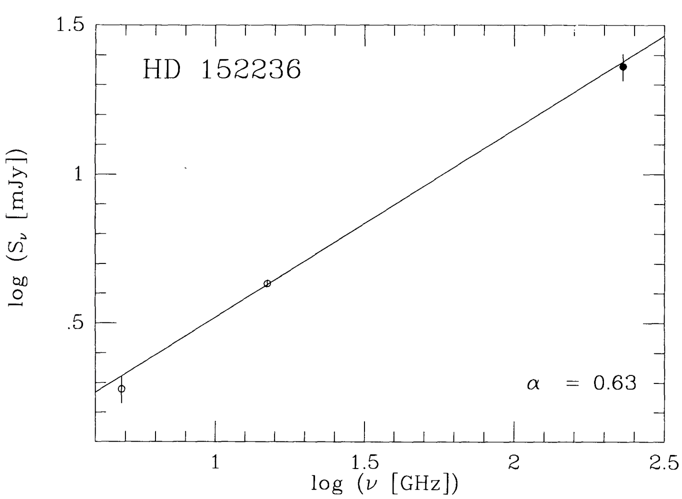

FIG. 6.—Same as Fig. 1 but for HD 152236. Filled circle: our millimeter data; open circles: Bieging et al. (1989). Spectral index: 0.63 ± 0.04.

Equation (2) can be used to derive the mass-loss rates from the observed 1.3 mm fluxes if d and v_∞ are known and if the chemical composition and ionization structure of the wind are specified. Spectral types of the program stars were taken from Humphreys (1978) for OB stars and from van der Hucht et al. (1981) for W-R stars (Table 2, col. [2]).

Column (3) of this table lists the stellar distances and the adopted uncertainties. They were derived assuming cluster membership in Ori OB1 for HD 37128 and Sco OB1 for HD 151932, HD 152236, and HD 152408, respectively (Humphreys 1978). The distance of HD 66811 and HD 68273 follow from the reasonable assumption that the two stars are the ionizing sources of the Gum Nebula (Brandt et al. 1971). HD 50896 is not member of a known cluster. We adopt the distance derived by Schmutz & Howarth (1991) from the strength of the interstellar absorption lines in HD 50896.

The terminal velocities of the winds in all program stars (col.

TABLE 2

PHYSICAL PARAMETERS OF THE PROGRAM STARS

Object (1)	Spectral Type (2)	d (kpc) (3)	v_∞ (km s^{-1}) (4)	T_e (K) (5)	μ (6)	Z (7)	γ (8)	g_ν (9)	log $\dot{M}_{1.3}$ ($M_\odot$ yr^{-1}) (10)
HD 37128	B0Ia	0.50 ± 0.1	1910	10000	1.6	1.0	1.0	2.96	−5.31 ± 0.16
HD 50896	WN5	1.8 ± 0.3	1720	10000	4.0	1.0	1.0	2.96	−4.11 ± 0.19
HD 66811	O4f	0.45 ± 0.1	2485	18000	1.5	1.2	1.2	3.33	−5.30 ± 0.17
HD 68273	WC8+O9I	0.45 ± 0.1	1415	10000	5.4	1.2	1.2	2.85	−4.05 ± 0.20
HD 151932	WN7	1.9 ± 0.2	1365	10000	2.2	1.0	1.0	2.96	−4.50 ± 0.17
HD 152236	B1.5Ia$^+$	1.9 ± 0.2	390	7000	1.6	0.9	0.8	2.73	−4.83 ± 0.11
HD 152408	O8fpe	1.9 ± 0.2	955	13000	1.5	1.0	1.0	3.18	−4.75 ± 0.12

© American Astronomical Society • Provided by the NASA Astrophysics Data System

1991ApJ...377..629L

[4]) were obtained from the violet limit of zero residual intensity in saturated ultraviolet P Cygni profiles (Prinja, Barlow, & Howarth 1990). We assume an error of 10% for v_∞. The terminal velocity of HD 68273 refers to the W-R component of the binary system. It is estimated from the C IV λ1550 line which shows v_∞ of the winds of the W-R—as well as of the O component. The value of v_∞ derived from C IV agrees well with the value determined by Barlow, Roche, & Aitken (1988) from the [Ne II] λ12.8 μm ($v_\infty = 1520$ km s^{-1}). We assume that the observed millimeter flux of HD 68273 is due to the wind from the W-R component. Conti & Smith (1972) derived $M_V = -6.2$ for the O component of the system. Using the average $\dot{M}$ versus luminosity relation of Garmany & Conti (1984), we expect a 1.3 mm flux of less than 5 mJy from the O star. This is negligible in comparison with the total radio flux measured for HD 68273.

Drew's (1989) models for the thermal equilibrium in O star winds demonstrated the importance of radiative and adiabatic cooling. Radiative losses in metallic lines and the H and He continuum and adiabatic cooling decrease the equilibrium temperature to less than 50% at $r = 10\,R_*$ relative to T_e at the stellar photosphere. The values of T_e for OB stars in Table 2 are based on $T_e = 0.4 T_{\rm eff}$ with the effective temperature derived from Schmidt-Kaler's (1982) calibration. Hillier (1988, 1989) investigated the temperature structure of WN and WC stars and found very low electron temperatures due to strong cooling in nitrogen and carbon lines. Hillier's models suggest $T_e \simeq 10^4$ K in those wind regions where millimeter radiation is predominantly emitted. We adopted 10^4 K for all W-R stars in our sample (see col. [5] of Table 2). Note that the electron temperature of the wind is of very minor importance for the calculated free-free flux: for example, varying T_e from 20,000 to 10,000 K decreases S_ν only by 13%.

Bohannan et al. (1986) found a helium overabundance of a factor of 2 relative to Galactic abundances in the atmosphere of HD 66811 ($Y = 0.17$) so that $\mu = 1.5$. Hydrogen and helium in early O stars can be expected to be in the form H^+ and He^{2+} within $r < 10\,R_*$ (Drew 1989), and therefore $Z = 1.2$, $\gamma = 1.2$. No detailed analysis has been done for HD 152408. Its evolutionary state suggests similar abundances as in HD 66811. On the basis of Drew's models we expect helium to be predominantly singly ionized beyond 10 R_*. Therefore we have $\mu = 1.5$ and $Z = \gamma = 1.0$ in HD 152408.

A significant helium overabundance has also been established for HD 37128 ($Y = 0.20$; Kudritzki et al. 1991). This leads to $\mu = 1.6$. We assume that hydrogen is fully ionized and all helium is He^+, that is, $Z = \gamma = 1.0$. HD 152236 lacks an analysis of its composition. As we did in the case of HD 152408, we assume the evolutionary status of HD 152236 to be similar to HD 37128 and use $\mu = 1.6$. Drew (1985) finds that helium starts recombining at $\sim 10\,R_*$ in P Cygni. The spectral similarity of HD 152236 to P Cygni suggests that neutral helium should also be dominating in HD 152236. Therefore we adopt $Z = 0.9$ and $\gamma = 0.8$.

Derivation of μ, Z, and γ is less straightforward in the case of W-R stars where the chemical composition and the ionization state of the wind are less well known. Models for HD 50896 by Hillier (1987a) and Schmutz (1990, private communication) give a small value for the recombination radius $R_{\rm rec}$ of He^{2+} into He^+. They find $R_{\rm rec} \approx 30$–$37\,R_*$ depending on the value of the core radius from the distance estimation. Therefore we assume that helium is mainly singly ionized in the 1.3 mm zone of emission which is believed to be localized further out in the wind than $R_{\rm rec}$. No hydrogen is expected to be present in the envelope of this WNE star. This is consistent with Hillier's (1987b) observations which derived $H^+/He^{2+} < 0.3$. Abundances for carbon and nitrogen were taken from Hillier (1988): N/He = 0.004, C/N = 0.07, and $N^{2+}/N^{3+} = 0.3$. This gives $\mu = 4.0$, $Z = 1.0$, and $\gamma = 1.0$.

The chemical composition and ionization structure of HD 68273 has been investigated by Barlow, Smith, & Willis (1981), Smith & Hummer (1988), and Torres (1988). Using the results from these studies and from Hillier's (1989) models for WC stars, we adopt C/He = 0.2 and assume that helium is entirely in the form of He^+ and that carbon is C^{2+} in the wind zone where 1.3 mm radiation originates. We calculate $\mu = 5.3$, $Z = 1.2$, and $\gamma = 1.2$. The ionization fractions are an extrapolation from what is observed in the wind regions closer to the star where recombination lines are formed. Smith & Hummer and Torres derived significant contributions of He^{2+} and C^{3+} from their recombination-line analysis. Although it is reasonable to expect recombination to occur inside the 1.3 mm zone (cf. Hillier's models), our assumption of complete recombination to He^+ and C^{2+} may be too simplistic. In fact, we will give arguments in § 5 that small fractions of He^{2+} and C^{3+} may still be present in the region of 1.3 mm emission. Nevertheless, we find that the derived mass-loss rate is rather insensitive to the actual fraction of He^{2+} and C^{3+}—*as long as* He^+ *and* C^{2+} *are the dominant ionization stages.*

For the WN7 star HD 151932, we took H/He = 1.5 based on the observations of Niedzielski (1989) and Conti, Leep, & Perry (1983) who all found H/He = 1–2 for the optically thin or thick case, respectively. As we did for the other WN star in our sample, HD 50896, we assume that He^+ dominates in the wind region sampled by the 1.3 mm flux ($R_{\rm rec} \simeq 10\,R_*$ for HD 151932; Schmutz 1990, private communication). This leads to $\mu = 2.2$, $Z = 1.0$, and $\gamma = 1.0$.

Errors on the abundance ratios and ionization fractions for W-R stars are large due to poor observational data and uncertain theoretical models. For instance, little is known about N and C abundances for HD 151932. Accordingly, uncertainties of 20% were adopted for μ, Z, and γ for the W-R stars. The uncertainties are smaller in OB stars where we take 10% for the errors in μ, Z, and γ. Columns (6), (7), and (8) of Table 2 summarize our results for the abundances and ionization states of the program stars.

Column (9) of Table 2 gives the Gaunt factors calculated with equation (3). Mass-loss rates derived from the observed millimeter fluxes are listed in column (10) of this table. The errors associated with $\dot{M}$ were calculated with

$$\sigma(\log \dot{M}) = \{[0.75\,\sigma(\log S_\nu)]^2 + [\sigma(\log v_\infty)]^2 + [1.5\,\sigma(\log d)]^2 + [\sigma(\log \mu)]^2 + [\sigma(\log Z)]^2 + [0.5\,\sigma(\log \gamma)]^2\}^{1/2} . \quad (4)$$

The errors for S_ν are taken from Table 1 and include only the measurement errors. As discussed before, there may be an additional uncertainty in S_ν at the 10% level due to the absolute flux calibration at 1.3 mm. The dominant error in the derived mass-loss rates is due to the uncertain distances of the program stars. Although all stars (except HD 50896) are members of clusters or associations, their distances are uncertain by 10%–20%. Presently the distance uncertainty sets the limit for the accuracy of $\dot{M}$ derived from radio data.

© American Astronomical Society • Provided by the NASA Astrophysics Data System

1991ApJ...377..629L

5. IMPLICATIONS FOR THE WIND PROPERTIES OF MASSIVE STARS

As expected from the general agreement between the theoretical and observational spectral indices, the mass-loss rates derived from the 1.3 mm fluxes compare well with the rates previously inferred from centimeter data (see Abbott et al. 1980, 1986; Bieging et al. 1989). The characteristic radius of emission R_ν where free-free radiation typically originates is given by

$$R_\nu = 2.8 \times 10^{28} T_e^{-1/2} (\gamma g_\nu)^{1/3} \left(\frac{\dot{M} Z}{\mu v_\infty \nu} \right)^{2/3} \quad (5)$$

(Panagia & Felli 1975; Wright & Barlow 1975); R_ν in cm and T_e in K; all other units are as in equation (2). The characteristic radius roughly scales like $R_\nu \propto \nu^{-2/3}$ so that observations at shorter radio wavelengths sample regions closer to the stellar surface.

Values for $R_\nu^{1.3\text{mm}}$, the radius of 1.3 mm emission of the program stars, are given in column (3) of Table 3. Transformation from absolute radius units to relative units was done using the stellar radii tabulated in column (2). R_* of OB stars is from Leitherer (1988). The stellar radii of W-R stars are from Schmutz, Hamann, & Wessolowski (1989). In the case of HD 68273, we used the average radius of the WCL stars presented in that paper. The value R_* of the W-R stars refers to the radius where the expansion velocity of the stellar wind is comparable to the local sound speed. This radius is typically smaller than the radius where the optical continuum of W-R stars is formed. We chose this definition of R_* for consistency reasons with the thermal equilibrium and ionization models discussed above, which used the same definition of the core radius of a W-R star.

We also calculated the radius of 6 cm emission $R_\nu^{6.0\text{ cm}}$ (col. [4] of Table 3). Unlike the relation between S_ν and $\dot{M}$ (eq. [2]), the characteristic radius depends on the electron temperature of the wind. For simplicity we assumed that T_e at $r = R_\nu^{6.0\text{ cm}}$ is the same as at $r = R_\nu^{1.3\text{ mm}}$. This may underestimate the actual radius of 6 cm emission since T_e will possibly decrease further out. In addition, the values of $R_\nu^{6.0\text{ cm}}$ were derived under the assumption that Z and γ are the same as those corresponding to $R_\nu^{1.3\text{ cm}}$. The consequences of relaxing this assumption of the radio spectrum will be discussed below.

Comparison of the characteristic radii at 1.3 mm and 6 cm demonstrates the importance of measurements at millimeter wavelengths. The value of $r = R_\nu^{1.3\text{ mm}}$ is approximately a factor of 15 smaller than $r = R_\nu^{6.0\text{ cm}}$. It coincides with (or is close to) wind regions which are accessible to alternative indicators of the wind structure, such as ultraviolet resonance lines in OB stars (Prinja et al. 1990) or optical recombination lines in W-R stars (Schmutz et al. 1989). The agreement between the theoretical spectral index predicted by equation (2) and the observed one from 1.3 mm to 6 cm suggests that the extrapolation of the electron density derived by spectroscopic means in near-photospheric regions to $r = R_\nu^{6.0\text{ cm}}$ is basically correct. In particular, no velocity gradients which are large enough to produce *significant* deviations from $\alpha = 0.6$ are observed. The value v_∞ as measured in ultraviolet absorption lines or optical recombination lines gives a good approximation of the wind velocity in the radio region. Consequently, $\dot{M}$ derived from the free-free flux at radio wavelengths using v_∞ should be expected to be close to the actual stellar mass-loss rate.

In the following sections we will discuss possible mechanisms affecting the theoretical free-free spectrum and assess their observational significance.

TABLE 3

CHARACTERISTIC RADIUS OF EMISSION

Object (1)	R_* ($R_\odot$) (2)	$R_\nu^{1.3\text{ mm}}$ (R_*) (3)	$R_\nu^{6.0\text{ cm}}$ R_*) (4)
HD 37128	35	6	91
HD 50896	5	155	2385
HD 66811	17	10	154
HD 68273	11	87	1342
HD 151932	28	27	408
HD 152236	98	13	198
HD 152408	30	24	372

5.1. *Nonthermal Contribution*

White (1985) showed that the nonthermal radio spectrum produced by synchrotron emission from chaotic stellar winds may resemble the thermal free-free spectrum. Depending on the choice of model parameters, the nonthermal spectrum, a spectral index between 0 and 0.5 is predicted. Observations of hot stars with nonthermal radio emission (Abbott, Bieging, and Churchwell 1984; Bieging et al. 1989) generally suggest $\alpha \leq 0$ at centimeter wavelengths. Although our program stars were selected on the basis of the absence of nonthermal emission, a small nonthermal contribution at longer wavelengths might have gone undetected.

Phase-dependent nonthermal radio emission may not be unexpected for the W-R binaries in our sample. Spectroscopic observations suggest that HD 50896 is probably a binary system where the unseen secondary is a neutron star (Firmani et al. 1980). In such a model, nonthermal emission might be generated by accretion of wind material from the W-R component on the compact companion (Moffat et al. 1982).

HD 68273 is a well-studied spectroscopic binary with a period of 78.5 days (e.g., Conti & Smith 1972; Moffat et al. 1986; Niemela & Sahade 1980). The winds of the two components might be expected to collide and produce shocks emitting nonthermal radio radiation. Williams et al. (1990) failed to detect nonthermal emission at 1.1 mm in HD 68273. Their measurements were performed at a phase of $\phi \simeq 0.75$. The phase angle of the system at the time of our observations was $\phi \simeq 0.3$. A comparison of our results with those of Williams et al. indicates no significant phase-dependent flux variation. Since the relative contribution of nonthermal emission should be different at different phases, this suggests that nonthermal emission is not detected at millimeter wavelengths. However, observations covering a wider range of phases, especially 0.0 and 0.5, would be desirable. The observational uncertainties associated with the spectral index do not allow us to prove or disprove the presence of significant nonthermal wind emission at centimeter wavelengths. However, given the shape of the nonthermal versus the thermal radio spectrum, we estimate that the contribution of nonthermal emission at 1.3 mm is negligible and $\dot{M}$ derived from the 1.3 mm fluxes is not affected by nonthermal emission.

5.2. *Deviations from Spherical Symmetry*

The consequences of deviations from spherical symmetry on the emerging free-free spectrum have been studied by Schmid-

© American Astronomical Society • Provided by the NASA Astrophysics Data System

1991ApJ...377..629L

Burgk (1982). Stationary, nonspherically symmetric outflows do not change the spectral index of the radio spectrum from 0.6. Therefore spectra with $\alpha \neq 0.6$ cannot be interpreted in terms of geometry effects. Vice versa, on the basis of the observed spectral index we cannot exclude the possibility that some of our program stars have asymmetric wind structures.

Spectropolarimetric observations of HD 50896 obtained by McLean et al. (1979) can be interpreted in terms of a flattened envelope. For the same object, Schulte-Ladbeck et al. (1990) found evidence for a rotating, expanding disk around a single star on the basis of He II $\lambda 4686$ polarization profiles. Even if such nonspherically symmetric structures are present, their effect on the derived mass-loss rates would be small. Only if some ratio of structural length scales in the wind exceeds ~ 10, the mass-loss rates would have to be corrected by a factor of ~ 2 as compared to the spherically symmetric case.

5.3. *Inhomogeneities and Time-Variability*

Observations of narrow components in ultraviolet resonance lines of OB stars (Prinja et al. 1990) and of fine structure in the emission lines of W-R stars (McCandliss 1988; Moffat et al. 1988; Robert 1991) suggest local density enhancements in these stars. The existence of such density enhancements questions the validity of equation (2), which was derived under the assumption of homogeneity and stationarity.

Clumps distributed uniformly throughout the wind have no influence on the spectral index (Abbott et al. 1981). They affect the free-free flux in the same way at all frequencies. Severe clumping in the wind would lead to an overestimate of $\dot{M}$ derived from equation (2). Abbott et al. (1981) showed that a noticeable effect is only produced if nearly all of the wind material is confined to high-density regions occupying a small fractional wind volume. This situation is not in agreement with spectroscopic observations which suggest that only a small mass fraction of the stellar outflow occurs in larger blobs (Robert 1991). We conclude that spatial inhomogeneities do not significantly affect the radio flux.

Time-dependent mass loss modifies the free-free spectrum. A high-density shell in P Cygni resulting from a mass-loss rate temporarily increased by a factor of 2 steepens the radio spectrum by ~ 0.1 during a time interval comparable to the flow time scale (Abbott et al. 1981). The reason for the relatively modest effect is the combination of the enhanced emission of the shell and its shadowing of other wind regions due to increased optical depth. The net result is that the radio flux is relatively insensitive to a variable mass-loss rate.

Probably some of the radio variability discussed in § 3 can be ascribed to a stellar mass-loss rate varying with time. On the other hand, careful long-term monitoring of individual stars like HD 50896 (Hogg 1989) revealed no significant flux variation above the 20% level. This is consistent with the model calculations of Abbott et al. (1981) described above. Mass-loss variations by large factors may occur in P Cygni–type stars, but such variations are not observed in OB and W-R-stars (see Lamers 1988). Therefore we do not expect that α will differ by more than ~ 0.05 from its classical value of 0.6 due to mass-loss variability. Such an effect will be difficult to detect given the present uncertainties of observed radio fluxes.

5.4. *Temperature Structure*

The theoretical radio spectrum of equation (2) was derived for an isothermal outflow with constant velocity and ionization throughout the wind. It can be generalized for outflows with a power-law dependence of T_e, v, Z, and γ on the radial distance from the star, that is,

$$T_e(r) \propto r^{-\delta} , \quad (6)$$

$$v(r) \propto r^{\epsilon} , \quad (7)$$

$$Z(r) \propto r^{-\zeta} , \quad (8)$$

$$\gamma(r) \propto r^{-\eta} ; \quad (9)$$

$\delta \geq 0$, $\epsilon \geq 0$, $\zeta \geq 0$, $\eta \geq 0$. Using the results by Wright & Barlow (1975) and Schmid-Burgk (1982), it can be shown that the radio spectral index becomes

$$\alpha = \frac{-0.6\delta + 4\epsilon + 4\zeta + 2\eta + 1.8}{-1.35\delta + 2\epsilon + 2\zeta + \eta + 3} . \quad (10)$$

Note that this expression for α already contains the ν–dependence of the Gaunt factor so that $S_\nu \propto \nu^{0.6}$ is retained if $\delta = \epsilon = \zeta = \eta = 0$. Equation (10) implies that any decrease of the electron temperature or the ionization state with radius or an increase of $v(r)$ will steepen the radio spectrum. We will first investigate the influence of the electron temperature.

The models for the thermal equilibrium in stellar winds discussed in § 3 predict a decrease of T_e with distance. The computed temperature profiles suggest that most of the cooling occurs within a few R_* due to radiative losses. Further out in the wind the temperature asymptotically reaches a constant value. Hogg (1985) derived $T_e \simeq 6000$ K by resolving the wind of HD 68273 at 6 cm. Assuming a conservative upper limit of $\delta < 0.25$ between the wind regions where the centimeter and millimeter fluxes originate, we find with equation (10) that α will be increased by less than 0.02. Unless substantially higher temperature gradients occur, variations of T_e with r are not noticeable in the radio spectrum.

5.5. *Influence of Acceleration or Deceleration Zones*

A fundamental assumption inherent in equation (2) is the absence of any acceleration and deceleration zones in the wind between the regions of millimeter and centimeter radiation emission. The theory of radiatively driven winds predicts a wind velocity law rising sharply close to the stellar surface with negligible acceleration beyond $r > 5\ R_*$. The value of $v(r)$ is usually parameterized as

$$v(r) = v_\infty \left(1 - \frac{R_*}{r}\right)^\beta , \quad (11)$$

with β between 0.5 and 1 (Castor et al. 1975; Kudritzki et al. 1991). Observational support for such a velocity law in O stars comes from, for example, Hα (Leitherer 1988) or UV resonance lines (Groenewegen & Lamers 1989). Equation (11) with $\beta = 1$ predicts essentially no acceleration between the regions where millimeter and centimeter radiation is emitted. For instance, the wind of HD 66811 expands with a velocity of $0.9v_\infty$ at $R_\nu^{1.3\ \mathrm{mm}}$ and reaches v_∞ at $R_\nu^{6\ \mathrm{cm}}$ if $\beta = 1$. Using equations (10) and (5) we find that this leads to a theoretical spectral index of 0.64 between 1.3 mm and 6 cm instead of 0.6 in the case of constant expansion velocity. Assuming that equation (11) with $\beta = 1$ is a valid representation for OB star winds in general, we would therefore expect that the observed radio spectrum should be around $\alpha \simeq 0.65$. Such a trend may actually be present in our sample of program stars, but it is difficult to disentangle from other effects such as changes in the ionization structure of the wind (see below).

© American Astronomical Society • Provided by the NASA Astrophysics Data System

1991ApJ...377..629L

The velocity field of the winds of W-R stars is still under investigation. It is not clear if radiation pressure is the mass-loss mechanism driving the outflow from these objects (see Abbott & Conti 1987 for a discussion), and no reliable theoretical predictions for $v(r)$ are available. Schmutz et al. (1989) find good agreement between observational and theoretical spectral-line strengths with $\beta = 1$. On the other hand, empirical mapping of the velocity field of V444 Cygni (Koenigsberger & Auer 1991) suggests significant acceleration zones beyond 10 stellar radii and correspondingly $\beta > 1$. Further evidence for a relatively gradual $v(r)$ comes from time-resolved high-resolution spectroscopy of W-R line profiles (Robert 1991). Such observations demonstrate the existence of blobs in the wind which can be used to sample the velocity field. Moffat & Robert (1991) showed that the observed propagation trajectories are understandable if β is larger than unity.

The spectral indicates found here for the W-R stars do not indicate any substantial deviation from the case of $\alpha = 0.6$. Assuming only acceleration or deceleration zones are responsible for deviations of α from the model described by equation (2), a lower limit for the ratio of the wind velocities at $R_v^{1.3\ \mathrm{mm}}$ and $R_v^{6\ \mathrm{cm}}$, $v_{1.3\ \mathrm{mm}}/v_{6\ \mathrm{cm}}$, can be derived. Since $\alpha < 0.75$ in all program stars (see Table 1), one finds $v_{1.3\ \mathrm{mm}}/v_{6\ \mathrm{cm}} > 0.65$. This lower limit for $v_{1.3\ \mathrm{mm}}/v_{6\ \mathrm{cm}}$ most probably underestimates the actual limit since we did not take the influence of different ionization zones in the wind into account. We will demonstrate in the following paragraph that such ionization zones will also steepen the radio spectrum. In any case, our observational data suggest that velocity gradients between $R_v^{1.3\ \mathrm{mm}}$ and $R_v^{6\ \mathrm{cm}}$ are not large enough to significantly affect mass-loss rates previously derived from 6 cm fluxes under the assumption of negligible acceleration between $R_v^{1.3\ \mathrm{mm}}$ and $R_v^{6\ \mathrm{cm}}$.

5.6. *Variation of the Ionization State with Distance*

Ionization conditions in the wind affect the emitted free-free spectrum in a twofold way: the mean ionic charge and the number of electrons per ion are modified. Such effects become more and more important with decreasing hydrogen content of the star. Hydrogen can always be assumed to be completely ionized in hot stars, whereas the ionization states of helium and heavy elements require more detailed modeling. Modifications of the adopted ionization conditions and abundances in W-R stars have led to an upward revision of the derived 6 cm mass-loss rates by factors of ~ 3 (Schmutz & Hamann 1986; van der Hucht, Cassinelli, and Williams 1986).

In general, the ionization conditions shift toward lower ionization further out in the wind so that Z and γ decrease with r. It follows from equation (10) that the spectral index will increase as compared to the case of constant Z and γ. Helium is the most likely element to affect Z and γ. Its abundance is high enough to be important for the mean ionic charge and to provide a significant number of free electrons, and its ionization potential lies in the critical range so that wind models predict noticeable variations of He^{2+}/He^{+} for the parameter space applicable in our program stars.

We will concentrate in our discussion on HD 66811 and HD 68273 since these two objects have spectral indices significantly above 0.6. Other objects from our sample may also have $\alpha > 0.6$, but the observational errors—as well as possible systematic effects due to the absolute calibration—are too large to rule out radio spectra with $\alpha = 0.6$ in those cases. Drew's (1989) thermal equilibrium models suggest that helium should be predominantly doubly ionized in HD 66811 at $r \simeq R_v^{1.3\ \mathrm{mm}}$ but recombination to He^{+} will occur further out. If helium is doubly ionized at $R_v^{1.3\ \mathrm{mm}}$ and singly ionized at $R_v^{6\ \mathrm{cm}}$ in the wind of HD 66811, we calculate $\alpha = 0.70$ with equations (10) and (5). This value of α agrees rather well with the observed spectral index of 0.71 ± 0.03. We may slightly overestimate the theoretical spectral index due to the assumption of $He^{2+} \gg He^{+}$ at $R_v^{1.3\ \mathrm{mm}}$. The radius where He^{2+} starts to recombine to He^{+} depends critically on the model parameters and should be close to $R_v^{1.3\ \mathrm{mm}}$. Consequently, He^{+} might not be completely negligible at $R_v^{1.3\ \mathrm{m}}$, and the theoretical spectral index will be $0.60 < \alpha < 0.70$. We conclude that the observed spectral index of HD 66811 can most likely be understood by a combination of two effects steepening the spectrum with respect to the case of equation (2): recombination of helium and some small acceleration of the outflow $0.9v_\infty$ to v_∞ as discussed in the preceding paragraph.

The ionization structure of HD 68273 is less straightforward to predict. We assumed that helium is entirely in the form of He^{+} at $R_v^{1.3\ \mathrm{mm}}$, and carbon is C^{2+}. As already mentioned in § 3, this assumption may slightly underestimate the degree of ionization at $R_v^{1.3\ \mathrm{mm}}$. If some He^{2+} and C^{3+} is still present at $R_v^{1.3\ \mathrm{mm}}$ and gradually recombines to He^{+} and C^{2+} at $R_v^{6\ \mathrm{cm}}$, a steepening of the spectral index can be produced like in the case of HD 66811. Such an effect has also been suggested by Williams et al. (1990). In addition, we expect some extended acceleration zones in the millimeter region, which may be more important in W-R stars than in OB stars. Therefore we interpret the observed spectral index of HD 68273 in terms of changes in the ionization structure *and* velocity gradients.

6. CONCLUSIONS

Measurements of hot stars at a wavelength of 1.3 mm provide accurate values of stellar mass-loss rates. As compared to measurements at centimeter wavelengths, millimeter fluxes sample wind regions which are also accessible to other spectroscopic mass-loss indicators, such as ultraviolet resonance lines or strong optical recombination lines. On the other hand, millimeter radiation originates sufficiently far outside the rapid acceleration zone of the stellar wind so that mass-loss rates can be derived without detailed modeling of $v(r)$. These favorable circumstances make mass-loss rates deduced from millimeter measurements quite independent from model assumptions inherent in other methods.

The "classical" theoretical spectral index for the free-free spectrum arising from an isotropic, isothermal outflow expanding at constant velocity is 0.6. The average spectral index of 0.63 derived for our sample of seven program stars is close to this canonical value. The agreement between the theoretical and observational values implies that the simple model adopted for the radiative transfer is correct. In particular, it can be excluded that *significant* acceleration zones exist in the wind between the regions where millimeter and centimeter radiation originate. Mass-loss rates which have previously been derived from measurement of the wind densities at centimeter wavelengths and with an extrapolation of the velocity field assuming $v(r) = constant$ are reliable.

We find no evidence for a systematic, large-scale, upward or downward revision of existing radio mass-loss rates. $\dot{M}$ from radio data is used to test the accuracy of other techniques to derive mass-loss rates in hot stars, such as Hα or ultraviolet resonance lines. Howarth & Prinja (1989) demonstrated that mass-loss rates from ultraviolet and radio data at centimeter wavelengths are in agreement. Leitherer (1988) calibrated Hα

© American Astronomical Society • Provided by the NASA Astrophysics Data System

1991ApJ...377..629L

mass-loss rates for galactic OB stars using ultraviolet rates. Our new results implying that the mass-loss rates derived from these different observational techniques are consistent and that the present calibration of observational mass-loss rates from radio fluxes, ultraviolet resonance lines, and Hα line fluxes is consistent and reliable. There is no indication that the average empirical relation between $\dot{M}$ and stellar parameters such as luminosity and effective temperature (e.g., Abbott 1985) needs substantial modification. These mass-loss rates are input for stellar evolution models of stars with solar metal content (Maeder 1990). Revisions of the empirical mass-loss rates by as little as 0.3 dex would have quite dramatic effects on the evolutionary tracks in the Hertzsprung-Russell diagram.

Although we find gross agreement between the observations and the isotropic, isothermal, constant-velocity model, there are indications that smaller, second-order effects affect the radio spectrum between 1.3 mm and 6 cm. Nonthermal contributions to the thermal emission, deviations from spherical symmetry, inhomogeneities, time variability, and temperature gradients do not produce observable effects in the radio spectra of our program stars. However, we find evidence for radio spectra with $\alpha \simeq 0.7$, which we interpret in terms of changes in the ionization structure and small velocity gradients in the wind. We find that an observed slope of the radio spectrum with $0.6 < \alpha < 0.7$ is in agreement with available models for the thermal equilibrium and the hydrodynamics of the wind. In principle, millimeter measurements are a very powerful tool to investigate such phenomena and to test theoretical models. However, it is difficult to seperate each of the effects individually unless other constraints on the models are available.

We find no significant difference between the radio spectra observed in OB and W-R stars except for the fact that the wind densities are generally higher in W-R stars. This may suggest that the physical conditions in those wind regions where radio radiation is emitted are rather similar. We do emphasize, however, that the important physical processes operating in stellar winds of OB and W-R stars may be very different. It is generally agreed that the theory of radiatively driven winds (Castor et al. 1975) provides an adequate description of an O star wind. The agreement between the theory and observations is generally quite good although systematic discrepancies of up to a factor of 2 may still exist. Kudritzki et al. (1991) found such disagreement between $\dot{M}$ calculated from the theory of radiatively driven winds and observational mass-loss rates from Hα (and consequently from the ultraviolet and radio). Despite these results, we believe that the theory of radiatively driven winds is an adequate model for winds of OB stars. Probably the disagreement can be explained by second-order effects such as time variability or deviations from spherical symmetry, which are not accounted for in the wind theory. In contrast, variability and inhomogeneities in stellar winds of W-R stars may well *not* be second-order effects. Although these phenomena hardly affect the free-free spectrum observed in the radio regime, they are evident from photometric, polarimetric, and spectroscopic observations. Studying and modeling these processes may ultimately provide the clue for understanding the properties of the winds of W-R stars.

We would like to thank Ernst Kreysa (MPIfR) and Lars-Åke Nyman (ESO) for their excellent support during the observing run. Thanks are due to Werner Schmutz who provided us with his W-R star models. We are grateful to Nino Panagia for stimulating discussions and for pointing out to us the approximation inherent in Allen's (1973) expression for the Gaunt factor. We are much obliged to Rolf Chini and Imke de Pater for information on the absolute flux calibration. We also appreciate useful discussions with Tony Moffat, Wan Chen, and Otto Richter. C. R. gratefully acknowledges financial support from the Visitor Fund of StScI and from the Université de Montréal.

APPENDIX

CALCULATION OF THE GAUNT FACTOR

Equation (3) follows from Spitzer's (1978) expression of the Gaunt factor for free-free transitions

$$g_\nu = \frac{\sqrt{3}}{\pi}\left[\ln \frac{(2kT_e)^{3/2}}{\pi e^2 \nu Z m_e^{1/2}} - \frac{5\tilde{\gamma}}{2}\right], \tag{A1}$$

which holds for $h\nu \ll kT_e$ and $\nu \gg \nu_p$. Boltzmann's constant is k; e is the electron charge; m_e is the electron mass; $\tilde{\gamma}$ is Euler's constant (0.577); and h is Planck's constant. The plasma frequency ν_p is given by

$$\nu_p = \left(\frac{n_e e^2}{\pi m_e}\right)^{1/2}, \tag{A2}$$

where n_e is the electron density. Equation (A1) is valid at millimeter and centimeter wavelengths under wind conditions in hot luminous stars. Allen (1973) gives for the free-free Gaunt factor,

$$g_\nu = 10.6 + 1.26 \log \frac{T_e^{3/2}}{\nu Z}. \tag{A3}$$

Allen's formula follows from equation (A1) if the term $5\tilde{\gamma}/2$ is neglected. This approximation has been used, for example, by Waters & Lamers (1984) in their tabulation of Gaunt factors for a large range of wavelengths and wind parameters. However, neglecting the term $5\tilde{\gamma}/2$ at a wavelength of 1.3 mm introduces an unnecessarily large error in g_ν. For instance, equation (A1) predicts $g_\nu = 2.96$ if $T_e = 10^4$ K and $Z = 1$, whereas Allen's approximation leads to $g_\nu = 3.84$.

© American Astronomical Society • Provided by the NASA Astrophysics Data System

1991ApJ...377..629L

We note that the expression for the free-free Gaunt factor given by van der Hucht et al. (1986) was derived from equation (A1). Their equation contains a typographical error: 17.22 should read 17.72. This, however, has negligible consequences for the calculated free-free flux.

REFERENCES

Abbott, D. C. 1985, in Radio Stars, ed. R. M. Hjellming & D. M. Gibson (Dordrecht: Reidel), 61
Abbott, D. C., Bieging, J. H., & Churchwell, E. 1981, ApJ, 250, 645
———. 1984, ApJ, 280, 671
Abbott, D. C., Bieging, J. H., Churchwell, E., & Cassinelli, J. P. 1980, ApJ, 238, 196
Abbott, D. C., Bieging, J. H., Churchwell, E., & Torres, A. V. 1986, ApJ, 303, 239
Abbott, D. C., & Conti, P. S. 1987, ARA&A, 25, 113
Allen, C. W. 1973, Astrophysical Quantities (London: Athlone), 103
Barlow, M. J., Roche, P. F., & Aitken, D. K. 1988, MNRAS, 232, 821
Barlow, M. J., Smith, L. J., & Willis, A. J. 1981, MNRAS, 196, 101
Bieging, J. H., Abbott, D. C., & Churchwell, E. 1989, ApJ, 340, 518
Bohannan, B., Abbott, D. C., Voels, S. A., & Hummer, D. G. 1986, ApJ, 308, 728
Brandt, J. C., Stecher, T. P., Crawford, D. L., & Maran, S. P. 1971, ApJ, 163, L99
Cassinelli, J. P., & Lamers, H. J. G. L. M. 1987, in Exploring the Universe with the IUE Satellite, ed. Y. Kondo (Dordrecht: Reidel), 139
Castor, J. I., Abbott, D. C., & Klein, R. I. 1975, ApJ, 195, 157
Conti, P. S., Leep, E. M., & Perry, D. 1983, ApJ, 268, 228
Conti, P. S., & Smith, L. F. 1972, ApJ, 172, 623
Drew J. E. 1985, MNRAS, 217, 867
———. 1989, ApJS, 71, 267
Firmani, C., Koenigsberger, G., Bissiacchi, G. F., Moffat, A. F. J., & Isserstedt, J. 1980, ApJ, 239, 607
Garmany, C. D., & Conti, P. S. 1984, ApJ, 284, 705
Groenewegen, M. A. T., & Lamers, H. J. G. L. M. 1989, A&AS, 79, 359
Hillier, D. J. 1987a, ApJS, 63, 947
———. 1987b, ApJS, 63, 965
———. 1988, ApJ, 327, 822
———. 1989, ApJ, 347, 392
Hogg, D. E. 1985, in Radio Stars, ed. R. M. Hjellming & D. M. Gibson (Dordrecht: Reidel), 117
———. 1989, AJ, 98, 282
Howarth, I. D., & Prinja, R. K. 1989, ApJS, 69, 527
Humphreys, R. M. 1978, ApJS, 38, 309
Jones, P. A. 1985, MNRAS, 216, 613
Koenigsberger, G., & Auer, L. H. 1991, in IAU Symp. 143, Wolf-Rayet Stars and Interrelations with Other Massive Stars in Galaxies, ed. K. A. van der Hucht & B. Hidayat (Dordrecht: Kluwer), 175
Kreysa, E. 1990, in Proc. 29th Liège Internat. Astr. Colloq., From Ground-Based to Space-Borne Sub-mm Astronomy, ed. B. Kaldeich (ESA SP-314), 265
Kudritzki R. P., Gabler, R., Kunze, D., Pauldrach, A. W. A., & Puls, J. 1991, in Massive Stars in Starbursts, ed. C. Leitherer, N. Walborn, T. Heckman, & C. Norman (Cambridge: Cambridge University Press), 59
Lamers, H. J. G. L. M. 1988, in Mass Outflows from Stars and Galactic Nuclei, ed. L. Bianchi & R. Gilmozzi (Dordrecht: Reidel), 39
Leitherer, C. 1988, ApJ, 326, 356
Maeder, A. 1990, A&AS, 84, 139
McCandliss, S. R. 1988, Ph.D. thesis, University of Colorado
McLean, I. S., Coyne, G. V., Frecker, J. E., & Serkowski, K. 1979, ApJ, 231, L141
Moffat, A. F. J., Drissen, L., Lamontagne, R., & Robert, C. 1988, ApJ, 334, 1038
Moffat, A. F. J., Firmani, C., McLean, I. S., & Seggewiss, W. 1982, in IAU Symp. 99, Wolf-Rayet Stars: Observations, Physics, Evolution, ed. C. W. H. de Loore & A. J. Willis (Dordrecht: Reidel), 577
Moffat, A. F. J., & Robert, C. 1991, in IAU Symp. 143, Wolf-Rayet Stars and Interrelations with Other Massive Stars in Galaxies, ed. K. A. van der Hucht & B. Hidayat (Dordrecht: Kluwer), 109
Moffat, A. F. J., Vogt, N., Paquin, G., Lamontagne, R., & Barrera, L. H. 1986, AJ, 91, 1386
Niedzielski, A. 1989, Acta. Astr., 39, 251
Niemela, V. S., & Sahade, J. 1980, ApJ, 238, 244
Olnon, F. M. 1975, A&A, 39, 217
Panagia, N., & Felli, M. 1975, A&A, 39, 1
Prinja, R. K., Barlow, M. J., & Howarth, I. D. 1990, ApJ, 361, 607
Purton, C. R., Feldman, P. A., Marsh, K. A., Allen, D. A., & Wright, A. E. 1982, MNRAS, 198, 321
Robert, C. 1991, Ph.D. thesis, Université de Montréal
Schmid-Burgk, J. 1982, A&A, 108, 169
Schmidt-Kaler, T. 1982, in Landolt-Börnstein, New Series, Group VI, Vol. 2b, ed. K. Schaifers & H. H. Voigt (Berlin: Springer), 1
Schulte-Ladbeck, R. E., Nordsieck, K. H., Nook, M. A., Magalhaes, A. M., Taylor, M., Bjorkman, K. S., & Anderson, C. M. 1990, ApJ, 365, L19
Schmutz, W., & Hamann, W.-R. 1986, A&A, 166, L11
Schmutz, W., Hamann, W.-R., & Wessolowski, U. 1989, A&A, 210, 236
Schmutz, W., & Howarth, I. D. 1991, in IAU Symp. 143, Wolf-Rayet Stars and Interrelations with Other Massive Stars in Galaxies, ed. K. A. van der Hucht & B. Hidayat (Dordrecht: Kluwer), 639
Smith, L. F., & Hummer, D. G. 1988, MNRAS, 230, 511
Spitzer, L. 1978, Physical Processes in the Interstellar Medium (New York: Wiley), 58
Torres, A. V. 1988, ApJ, 325, 759
Ulrich, B. L., Dickel, J. R., & de Pater, I. 1984, Icarus, 60, 590
van der Hucht, K. A., Cassinelli, J. P., & Williams, P. M. 1986, A&A, 168, 111
van der Hucht, K. A., Conti, P. S., Lundström, I., & Stenholm, B. 1981, Space Sci. Rev., 28, 227
Waters, L. B. F. M., & Lamers, H. J. G. L. M. 1984, A&AS, 57, 327
White, R. N. 1985, ApJ, 289, 698
Williams, P. M., van der Hucht, K. A., Sandell, G., & Thé, P. S. 1990, MNRAS, 244, 101
Williams, P. M., van der Hucht, K. A., van der Woerd, H., Wamsteker, W., Geballe, T. R., Garmany, C. D., & Pollock, A. M. T. 1987, in Instabilities in Luminous Early Type Stars, ed. H. J. G. L. M. Lamers & C. W. H. de Loore (Dordrecht: Reidel), 221
Willis, A. J., & Garmany, C. D. 1987, in Exploring the Universe with the IUE Satellite, ed. Y. Kondo (Dordrecht: Reidel), 157
Wright, A. E., & Barlow, M. J. 1975, MNRAS, 170, 41

© American Astronomical Society • Provided by the NASA Astrophysics Data System